7-dehydrocholesterol suppresses melanoma cell proliferation and invasion via Akt1/NF-κB signaling

JIA LIU[1,2*], FEILIANG ZHONG[1,2*], LEI CAO[1,2], RUIYING ZHU[1,2], JUNZE QU[1,2], LIN YANG[3], TINGTING CHEN[4], YUNLONG HU[5], YING WANG[1,2], MINGDONG YAO[1,2], WENHAI XIAO[1,2], CHUN LI[1,2], BO LI[1,2] and YINGJIN YUAN[1,2]

[1]Frontier Science Center for Synthetic Biology and Key Laboratory of Systems Bioengineering (Ministry of Education), Tianjin University; [2]Collaborative Innovation Center of Chemical Science and Engineering (Tianjin), School of Chemical Engineering and Technology, Tianjin University, Tianjin 300072; [3]Centre for Reproductive Medicine, Tianjin Medical University General Hospital, Tianjin 300041; [4]Department of Physiology, School of Basic Medical Sciences, Health Sciences Center, Shenzhen University, Shenzhen, Guangdong 518060; [5]Guangdong Provincial Key Laboratory of Regional Immunity and Diseases, Department of Pathogen Biology, Health Sciences Center, Shenzhen University, Shenzhen, Guangdong 518055, P.R. China

Received March 11, 2020; Accepted September 14, 2020

DOI: 10.3892/ol.2020.12261

Abstract. Melanoma is the most lethal cutaneous cancer with a high metastatic rate worldwide, causing ~55,500 deaths annually. Although the selective B-Raf oncogene serine/threonine-kinase (BRAF) inhibitors, dabrafenib and vemurafenib, have been approved for the treatment of BRAF-mutant metastatic melanoma, the 5-year survival rate remains unfavorable due to acquired therapy resistance. Therefore, it is of great importance to develop alternative therapeutic drugs and uncover their mechanisms for the treatment of melanoma. 7-dehydrocholesterol (7-DHC) has been demonstrated to inhibit melanoma, but the mechanism is unclear. Therefore, the present study aimed to elucidate the mechanisms of the inhibitory effect of 7-DHC in melanoma cells via analyzing the proliferation, migration, apoptosis, cell cycle and transcriptional sequencing of melanoma cells treated with 7-DHC, as well as constructing a gene signature according to public data of patients with melanoma. In the present study, 7-DHC, the precursor of vitamin D_3, was able to induce apoptosis and inhibit cell proliferation and invasion of melanoma cells in a dose-dependent manner. RNA sequencing of melanoma cells treated with different concentrations of 7-DHC revealed that, compared with untreated melanoma cells, 65 genes were downregulated, and genes involved in the regulation of NF-κB import into the nucleus and NF-κB signaling were significantly repressed. Consistently, the Akt kinase family was one of most common somatic mutation hotspots in patients with melanoma according to The Cancer Genome Atlas enrichment analysis. Furthermore, 7-DHC decreased the phosphorylation of Akt1-Ser473 rather than that of MEK1, and the decreased phosphorylation of Akt1 subsequently inhibited the translocation of free RELA proto-oncogene NF-κB subunit to the nucleus. Finally, by intersecting downregulated genes by 7-DHC treatment and upregulated genes in patients with melanoma, a 7-DHC gene signature was identified, which was negatively associated with the prognosis. Overall, the present results demonstrated that 7-DHC suppressed melanoma cell proliferation and invasion via the Akt1/NF-κB signaling pathway, and 7-DHC key target genes were negatively associated with the prognosis. These findings highlight the potential application of 7-DHC for the treatment of melanoma in the future.

Introduction

Melanoma, originating from melanocytes that produce melanin, is the most common type of skin cancer with a poor prognosis (1). Epidemiological studies demonstrated that ~55,500 people die of melanoma annually worldwide (2,3), and its incidence rate was the highest among Caucasians, particularly in New Zealand (0.0358%) and Australia (0.0349%) in 2012 (4). Clinically, melanoma lesions are classified according to their location and progression, ranging from benign nevi to metastatic melanoma (5). The exact cause of melanoma is unknown; however, exposure to ultraviolet radiation from sunlight increases the risk of developing melanoma (6). Additionally, genetic background and pigmentation status contribute to cancer predisposition (7-9). Melanoma can be

Correspondence to: Dr Bo Li, Frontier Science Center for Synthetic Biology and Key Laboratory of Systems Bioengineering (Ministry of Education), Tianjin University, 92 Wei Jin Road, Tianjin 300072, P.R. China
E-mail: lib028@tju.edu.cn

*Contributed equally

Key words: melanoma, 7-dehydrocholesterol, RNA sequencing, Akt1/NF-κB, prognosis

cured at the early stage; however, advanced melanoma easily metastasizes to lymph glands without cell adhesion between lymph nodes and other metastases, leading to treatment resistance and a poor prognosis (5). Before the approval of selective kinase inhibitors, such as dabrafenib, vemurafenib and trametinib, for metastatic melanoma in 2010 (10), the 5-year survival rate for patients with advanced melanoma was only 16% (11,12).

It is estimated that ~40% of melanoma cases contain oncogenic B-Raf oncogene serine/threonine-kinase (BRAF) somatic mutations, which lead to the constitutive activation of MAPK signaling and resistance to chemotherapy. The most common BRAF mutation is V600E, which accounts for ~5-90% of the BRAF mutations in melanoma (13). Since 2010, vemurafenib and dabrafenib targeting BRAF V600E have been approved for the treatment of patients with advanced melanoma in numerous countries around the world (10). Both progression-free survival and overall survival times are now extended in patients with metastatic melanoma with BRAF V600E mutation (14). However, the 5-year survival rates of melanoma remain unfavorable, due to resistance to treatment in most patients within ~12 months (12). Therefore, identification of novel therapeutic targets and understanding their molecular mechanisms are urgently required for melanoma therapy.

The precursor of vitamin D_3, 7-dehydrocholesterol (7-DHC), is stored under human skin and serves an important role in regulating calcium and phosphorus metabolism (13,15). 7-DHC has been demonstrated to be associated with numerous processes, such as the maintenance of the epidermal barrier and the treatment of common skin diseases (16). Recently, researchers revealed that 7-DHC treatment could specifically promote the phosphorylation of interferon regulatory factor 3 and enhance type I interferon production in macrophages, suggesting 7-DHC as a potential therapeutic agent against emerging or highly pathogenic viruses (17). In addition, in ovarian cancer, the replacement of cholesterol by 7-DHC efficiently enhances the anticancer activity of photosensitizer-encapsulated liposomes upon irradiation (18), and 7-DHC peroxide exhibits improved anticancer activity and selectivity over ergosterol peroxide (19). Although the mechanism has not been fully elucidated yet, 7-DHC has been demonstrated to elicit cytotoxic and apoptosis-promoting effects in melanoma cells (20).

In the present study, the transcriptome analysis of A375 cells with 7-DHC treatment and mutational hotspots of kinase-coding genes recorded in The Cancer Genome Atlas (TCGA) database were integrated to determine the molecular mechanism underlying the anticancer property of 7-DHC and provide a theoretical basis for its clinical application.

Materials and methods

Cell lines and cell culture. A375 malignant melanoma and 293T embryonic kidney cells were purchased from the China Infrastructure of Cell Line Resources (Institute of Basic Medical Sciences; Chinese Academy of Medical Sciences). A2058 melanoma cells were kindly provided by Dr Qiong Yang from the Fang Lab of the Beijing Institute of Genomics of the Chinese Academy of Sciences. All cells were maintained in high-glucose DMEM (Gibco; Thermo Fisher Scientific, Inc.) supplemented with 10% FBS (Gibco; Thermo Fisher Scientific, Inc.) and 1% penicillin-streptomycin (Beijing Solarbio Science & Technology Co., Ltd.) at 37˚C, 95% humidity and 5% CO_2.

Reverse transcription-quantitative PCR (RT-qPCR) assay. Total RNA was extracted from A375 and A2058 melanoma transfected cells or cells treated with the AKT1 inhibitor MK-2206 (1 μM; cat. no. HY-10358; MedChemExpress) or the AKT inhibitor III (1 μM; cat. no. HY-10355; MedChemExpress) using TRIzol® reagent (Invitrogen; Thermo Fisher Scientific, Inc.), and cDNA was produced using a reverse transcription kit (TransScript All-in-One First-Strand cDNA Synthesis SuperMix for qPCR; TransGen Biotech Co., Ltd.) at 42˚C for 15 min according to the manufacturer's protocol. qPCR was performed using SYBR PCR mix (TransGen Biotech Co., Ltd.) and GAPDH was used as the housekeeping gene for internal reference. The following primers were used to amplify genes at a concentration of 5 μM: RELA proto-oncogene NF-κB subunit (RELA; gene ID, ENSG00000173039) forward, 5'-TTCCGACCGGGAGCTCAGTG-3' [20 bp; melting temperature (Tm), 61˚C] and reverse, 5'-TGCGGGAAGGCACAGCAAT-3' (19 bp; Tm, 62˚C); long intergenic non-protein coding RNA 552 (LINC00552; gene ID, ENSG00000279770) forward, 5'-ACACAGACATGCACACACAGG-3' (21 bp; Tm, 60˚C) and reverse, 5'-GGGGCCAGTGGATTTTCATG-3' (20 bp; Tm, 58˚C); ADAM metallopeptidase domain 19 (ADAM19; gene ID, ENSG00000135074) forward, 5'-CGAGAAGGTGAATGTGGCAGGA-3' (22 bp; Tm, 61˚C) and reverse, 5'-AGCTCTGACACTGGATCTTCCC-3' (22 bp; Tm, 60˚C); C-X-C motif chemokine ligand 3 (CXCL3; gene ID, ENSG00000163734) forward, 5'-TCCGTGGTCACTGAACTGCG-3' (20 bp; Tm, 61˚C) and reverse, 5'-AGTTGGTGCTCCCCTTGTTCA-3' (21 bp; Tm, 60˚C); insulin-like growth factor binding protein 5 (IGFBP5; gene ID, ENSG00000115461) forward, 5'-ACCTGAGATGAGACAGGAGTC-3' (21 bp; Tm, 56˚C) and reverse, 5'-GTAGAATCCTTTGCGGTCACAA-3' (22 bp; Tm, 57˚C); MMP9 (gene ID, ENSG00000100985) forward, 5'-AACTACGACCGGGACAAGCTC-3' (21 bp; Tm, 60˚C) and reverse, 5'-ACAGGTCGAGTACTCCTTACCCAG-3' (24 bp; Tm, 60˚C); α-methylacyl-CoA racemase (AMACR; gene ID, ENSG00000242110) forward, 5'-AGAACCCCAGTTCTACGAGCTG-3' (22 bp; Tm, 60˚C) and reverse, 5'-ACTCTGCCTTCGTCTTCTCTGC-3' (22 bp; Tm, 61˚C); heme oxygenase 1 (HMOX1; gene ID, ENSG00000100292) forward, 5'-ACCCAGGCAGAGAATGCTGAG-3' (21 bp; Tm, 61˚C) and reverse, 5'-ACATAGATGTGGTACAGGGAGGC-3' (23 bp; Tm, 60˚C); IL11 (gene ID, ENSG00000095752) forward, 5'-TCCTGACCCGCTCTCTCCTG-3' (20 bp; Tm, 62˚C) and reverse, 5'-AGGGAATCCAGGTTGTGGTCC-3' (21 bp; Tm, 60˚C); lipocalin 2 (LCN2; gene ID, ENSG00000148346) forward, 5'-AGAGCTACAATGTCACCTCCGTC-3' (23 bp; Tm, 60˚C) and reverse, 5'-TCTTAATGTTGCCCAGCGTGAACT-3' (24 bp; Tm, 61˚C); prostaglandin-endoperoxide synthase 2 (PTGS2; gene ID, ENSG00000073756) forward, 5'-TACCCACTTCAAGGGATTTTGGAACG-3' (26 bp; Tm, 61˚C) and reverse, 5'-AGTCAGCATTGTAAGTTGGTGGACT-3' (25 bp; Tm, 61˚C); and GAPDH (gene ID, ENSG00000111640) forward, 5'-AGCCACATCGCTCAGACAC-3' (19 bp; Tm, 59˚C) and reverse, 5'-ACCAGGCGC

CCAATACGA-3' (18 bp; Tm, 60˚C). The qPCR thermocycling conditions were as follows: 94˚C for 30 sec, followed by 40 cycles of 5 sec at 94˚C for denaturation and 60˚C for 30 sec for annealing/extension using the two-step method. The expression fold changes were calculated using the $2^{-\Delta\Delta Cq}$ method (21).

Lentivirus packaging and infection. Three short hairpin RNAs (shRNAs) of RELA, namely shRNA-1 (5'-CGGATT GAGGAGAAACGTAAATTCAAGAGATTTACGTTT CTC CTCAATCCGTTTTTTG-3'), shRNA-2 (5'-GCCTTAATA GTAGGGTAAGTTTTCAAGAGAAACTTACCCTAC TAT TAAGGCTTTTTTG-3') and shRNA-3 (5'-GGATTCATT ACAGCTTAATTCAAGAGATTAAGCTGTAATGAA TCC ATTTTTTG-3'), and a scrambled control shRNA (5'-CGGTCC TAAGGTTAAGTCGCCCTCGCTCGAGCGAGGGCG ACT TAACCTTAGGTTTTTG-3'), were synthesized by Genewiz, Inc., and were then cloned into PLKO.1-EGFP-T2A-Puro (Addgene, Inc.) via *Age*I/*Eco*RI enzyme digestion sites. High titer production of lentivector was achieved by transiently co-transfecting 293T cells with lentiviral packaging plasmids, 4 μg pCMVR8.2, 1 μg pCMV-VSVG (Addgene, Inc.) and 3 μg RELA-shRNA-expressing constructs via Lipofectamine® 3000 (1 μl Lipofectamine 3000 per μg plasmid; Invitrogen; Thermo Fisher Scientific, Inc.). At 70-90% confluence, A375 melanoma cells were infected with the aforementioned shRNA lentiviruses with the help of Polybrene with a final concentration of 6 μg/ml (Sigma-Aldrich; Merck KGaA), according to the manufacturer's protocol. RNA was harvested 48 h post-infection to determine the knockdown efficiency using RT-qPCR, as aforementioned.

Cell proliferation assay. A375 cells treated with multiple concentrations (0, 1, 2.5, 5, 10 and 25 μM) of 7-DHC or infected with RELA-shRNA lentivirus, were cultured in a 96-well plate at a density of 5,000 cells/well at 37˚C for 48 h. Subsequently, 10 μl Cell Counting Kit-8 (APeXBIO Technology LLC) solution was added to each well and incubated at 37˚C with 5% CO_2 for another 4 h, according to the manufacturer's protocol. Absorbance was measured at a wavelength of 450 nm using an ELISA plate reader (Thermo Fisher Scientific, Inc.).

Apoptosis and cell cycle analysis using flow cytometry. A375 and A2058 cells were treated with ethanol (negative control) and different concentrations (1, 5 and 10 μM) of 7-DHC at 37˚C for 48 h and were then harvested at 500 g at 20˚C for 5 min and washed twice with PBS. Apoptosis was detected using the TransDetect Annexin V-FITC/PI Cell Apoptosis Detection kit (TransGen Biotech Co., Ltd.) according to the manufacturer's protocol; briefly, cells were resuspended with 100 μl Annexin V binding buffer and stained with 5 μl Annexin V-FITC and 5 μl PI for 20 min at room temperature. For cell cycles analysis, the cells were fixed with 70% ethanol at 4˚C overnight. On the next day, using the DNA Content Quantitation Assay kit (Beijing Solarbio Science & Technology Co., Ltd.), the cells were stained with 20 μl PI (50 μg/ml) and 20 μl RNase A (50 μg/ml) for 30 min at 4˚C. All samples were detected using a flow cytometer (NovoCyte 2040R; ACEA Bioscience, Inc.; Agilent Technologies) and analyzed using the NovoExpress 1.4.1 software (ACEA Bioscience, Inc.; Agilent Technologies).

Hoechst-PI double staining. A total of $5x10^5$ A375 and A2058 melanoma cells were cultured in 6-well plates at 37˚C for 48 h. During this period, some cells were treated with 25 μM 7-DHC, while negative control cells were treated with ethanol. Subsequently, 5 μl Hoechst and 5 μl PI staining solution from a Hoechst/PI double-staining kit (Beijing Solarbio Science & Technology Co., Ltd.) were added to the cells at 37˚C for 1 h. Finally, the plates were observed under a fluorescence microscope (eye lens x objective lens, 10x10; Leica S/N 443077; Leica Microsystems, Inc.).

Real-time cellular analysis (RTCA) assay. The migration rates of A375 and A2058 cells were analyzed using RTCA. A375 and A2058 cells were seeded into the upper chamber of individual CIM-Plate-16 (5,000 cells/well; ACEA Bioscience, Inc.; Agilent Technologies) in 130 μl DMEM without FBS. The upper chamber was then placed on the lower chamber of the CIM-Plate-16, which contained DMEM supplemented with 10% FCS as an attractant. Changes in impedance resulting from cells that had migrated to the bottom side of the membrane were recorded every 5 min and were monitored for a total of 36 h. Finally, the cell index values representing the migration rates were calculated using the xCELLigence 1.1 software (ACEA Bioscience, Inc.; Agilent Technologies, Inc.).

Chromatin immunoprecipitation (ChIP)-qPCR. ChIP experiments were performed using a SimpleChIP Plus Sonication Chromatin IP kit (Cell Signaling Technology, Inc.), according to the manufacturer's protocol. Normal rabbit IgG antibody was used as a control. Antibodies were as follows: Normal rabbit IgG (1:5,000; cat. no. 2729S; Cell Signaling Technology, Inc.) and anti-RELA (1:1,000; cat. no. ab19870; Abcam). Antibodies were incubated at 4˚C overnight. Subsequently, qPCR was performed using SYBR PCR mix kit (TransGen Biotech Co., Ltd.), and GAPDH was used as the reference gene. D130D1 was used as the negative control. The qPCR thermocycling conditions were as follows: 94˚C for 30 sec, followed by 40 cycles of 5 sec at 94˚C for denaturation and 60˚C for 30 sec for annealing/extension using the two-step method. The expression fold changes were calculated using the $2^{-\Delta\Delta Cq}$ method (21). Primers for RELA target genes promoter regions were as follows: LINC00552-P-1 forward, 5'-TCCATTATGAGCCCTGGGAC-3', and reverse, 5'-TCCCGGAGCCTCATTGATAC-3'; LINC00552-P-2 forward, 5'-GCTCTCTCACCATGCGATTG-3', and reverse, 5'-AGGCTGAGAAGTCCAAGGTC-3'; ADAM19-P-1 forward, 5'-GGCTTTGTTCCCACGTTCTG-3', and reverse, 5'-GAG GAAGGAGAAGGCGAGAA-3'; ADAM19-P-2 forward, 5'-TGGAAGAACACACGTCTGGT-3', and reverse, 5'-CTT TCCCCACACACCAAGC-3'; ADAM19-P-3 forward, 5'-TTT GTCGCCCAGGAGCAATA-3', and reverse, 5'-AGGGGATTT TGTCATGGGAAC-3'; CXCL1-P-1 forward, 5'-ATCCCAAAG TCCCAGAGTGC-3', and reverse, 5'-CAAGATCGGCGAACC CTTTT-3'; MMP9-P-1 forward, 5'-CAGTACCGAGAGAAA GCCTATT-3', and reverse, 5'-CAGGATGTCATAGGTCAC GTAG-3'; and GAPDH forward, 5'-AGCCACATCGCTCAG ACAC-3', and reverse, 5'-ACCAGGCGCCCAATACGA-3'.

Wound-healing assay. The A375 cell line is a typical malignant melanoma cell line, and therefore, wound-healing assays were performed in A375 cells to illustrate the inhibition

of migration by 7-DHC. A375 melanoma cells were cultured in six-well plates in DMEM with 10% FBS at 37˚C, 95% humidity and 5% CO_2 for 24 h until the cells reached 100% confluence. Subsequently, 200-μl sterile pipette tips were used to scratch the cells in the middle of each well. The medium of each well was discarded, PBS was added to wash cells and remove floating cells, and serum-free DMEM was added into each well. Different concentrations of 7-DHC were added into each well, with the final 7-DHC concentrations being 0, 1, 5, 10 and 25 μM. Wound-healing was observed and captured using a light inverted microscope at a magnification of 10x10 (eye lens x objective lens) at 0, 24 and 48 h. Lastly, the migration rate was evaluated by detecting the width of the cell-free region using GraphPad Prism 5 (GraphPad Software, Inc.) for the quantification and plotting.

Western blotting. Total protein lysates isolated from A375 and A2058 melanoma cells treated with different concentrations of 7-DHC (0, 1, 2.5, 5, 10 and 25 μM) or 1 μM insulin-like growth factor 1 (IGF1; Beijing Solarbio Science & Technology Co., Ltd.) at 37˚C for 48 h, were collected using RIPA buffer with a protease inhibitor cocktail (Beijing Solarbio Science & Technology Co., Ltd.). In addition, the nuclear and cytoplasmic proteins of A375 and A2058 cells were collected using the NE-PER Nuclear and Cytoplasmic Extraction Reagents kit (cat. no. 78835; Thermo Fisher Scientific, Inc.), according to the manufacturer's protocol. For western blotting, protein concentration was determined using a BCA assay and proteins (20 μg/lane) were separated via 12% SDS-PAGE and transferred onto a nitrocellulose membrane (EMD Millipore). The membrane was blocked with 5% skimmed milk in TBS-Tween (0.1% Tween 20) at room temperature for 1 h and then incubated at 4˚C overnight with primary antibodies against Akt1 (1:1,000; cat. no. 33224; Signalway Antibody LLC), phosphorylated (p) Akt1-Ser473 (1:1,000; cat. no. 13357; Signalway Antibody LLC), pAkt1-Thr308/309 (1:1,000; cat. no. 13311; Signalway Antibody LLC), MEK1 (1:1,000; cat. no. 21428; Signalway Antibody LLC), pMEK1-ser217/ser221 (1:1,000; cat. no. 11205; Signalway Antibody LLC), histone H3 (H3; 1:1,000; cat. no. ab1791; Abcam), RELA (1:1,000; cat. no. ab19870; Abcam), TUBULIN (1:5,000; cat. no. RM2007L; Beijing Ray antibody Biotech) and GAPDH (1:5,000; cat. no. ab181602; Abcam). After washing, the membrane was incubated with anti-mouse (1:5,000; cat. no. ab97040; Abcam) or anti-rabbit (1:5,000; cat. no. ab7090; Abcam) HRP-conjugated secondary antibodies at room temperature for 1 h. Bands recognized by antibodies were revealed using an ECL reagent (Thermo Fisher Scientific, Inc.) on Exposure meter Azure Imager 300 (Azure Biosystems, Inc.). Finally, ImageJ 1.52 software (National Institutes of Health) was used for quantification of protein expression.

Dual-luciferase assay. A375 melanoma cells were co-transfected with vectors of firefly luciferase and *Renilla* luciferase (Addgene, Inc.) using Lipofectamine 3000 (1 μl Lipofectamine 3000/μg plasmid; Invitrogen; Thermo Fisher Scientific, Inc.) at 37˚C for 48 h. Notably, the transcription of firefly luciferase was regulated by a mini-promoter constructed with 4 repeating RELA motifs (5'-GGGAAT TTCC-3'). The growth medium from the cultured cells was removed, and a sufficient volume of PBS was gently added to wash the surface of the culture vessel. The vessel was briefly swirled to remove the detached cells and residual growth medium, and PBS was removed. Subsequently, 1X passive lysis buffer from the dual-luciferase reporter assay system kit (cat. no. E1960; Promega Corporation) was added to each culture well, and the culture plates were rocked at room temperature for 15 min. A total of 100 μl Luciferase Assay Reagent II from the dual-luciferase reporter assay system kit (cat. no. E1960; Promega Corporation) was added to luminometer tubes including 20 μl lysate of samples. The absorbance was measured at a wavelength of 560 nm to detect the firefly luciferase activity. Stop & Glo Reagent (100 μl; Promega Corporation) was added to each tube, and the absorbance at a wavelength of 470 nm was measured to detect the *Renilla* luciferase activity. The luciferase results were determined via dividing the absorbance value of 560 nm by the absorbance value of 470 nm to normalize the firefly luciferase activity by the *Renilla* luciferase activity.

Bioinformatics analysis. R 3.5.1 software (https://www.r-project.org/) was used to analyze the RNA sequencing (RNA-seq) data of 7-DHC-treated (10 and 25 μM) A375 melanoma cells and the bioinformatics data from TCGA (https://www.cancer.gov/about-nci/organization/ccg/research/structural-enomics/tcga) and Gene-Tissue Expression (GTEX; http://genome.ucsc.edu/gtex.html) databases. Firstly, the limma 3.44.3 R package (http://www.bioconductor.org/packages/release/bioc/html/limma.html) was used to analyze the gene expression pattern of A375 cells treated with 7-DHC vs. ethanol to determine the differentially expressed genes [log fold change >1, adjusted (adj-)P<0.05]. ClusterProfiler 3.16.1 R package (http://www.bioconductor.org /packages/release/bioc/html/clusterProfiler.html) was used for the Gene Set Enrichment Analysis (GSEA) (22), which used the gene set c2.all.v6.2.entrez.gmt downloaded from the GSEA website (http://software.broadinstitute.org/gsea/downloads.jsp) for enrichment pathway, based on the aforementioned differential expression results.

Secondly, for the public data from TCGA and GTEX databases, the transcriptome data from 471 samples of patients with melanoma were downloaded from TCGA skin cutaneous melanoma (TCGA-SKCM) dataset and data from 813 normal skin samples were downloaded from the GTEX (http://genome.ucsc.edu/gtex.html) database. In order to compare the gene expression in normal and tumor samples, the RNA-seq data from TCGA and GTEX databases were normalized by log2 (fragments per kilobase of exon per million value) and the limma R package was used to analyze the gene expression pattern to screen for significantly differential genes (log fold change >1, adj-P<0.05).

Statistical analysis. Univariate and multivariate Cox proportional hazards regression analyses were performed, based on 19 genes of intersection between upregulated genes in melanoma tissues from TCGA-SKCM dataset and downregulated genes in melanoma cells treated with 7-DHC. Furthermore, a 5-gene prognosis predictive model was constructed, and patients with melanoma from TCGA-SKCM dataset were classified into high- and low-risk groups according to the mean value

of the risk score calculated using the survival 2.43 R package (https://CRAN.R-project.org/package=survivalAnalysis). The survivalROC 1.0.3 R package (https://cran.r-project.org/web/packages/survivalROC/index.html) was used to construct the time-dependent receiver operating characteristic (ROC) curve, in order to assess the sensitivity and specificity of the 5-gene signature in predicting survival. The Kaplan-Meier method and log-rank test were used to estimate the overall survival (OS). In addition, GraphPad Prism 5 (GraphPad Software, Inc.) was used for statistical analysis, and unpaired Student's t-test was used to compare the difference between two groups, while one-way ANOVA was used to compare differences among ≥3 groups, followed by Tukey's post hoc test. Data were presented as the mean ± standard deviation, and the experiments were repeated ≥3 times in each group. $P<0.05$ was considered to indicate a statistically significant difference.

Results

7-DHC increases apoptosis and inhibits proliferation and migration of melanoma cells. To confirm the anticancer property of 7-DHC on melanoma cells, proliferation assays were performed. Human embryonic kidney 293T cells and A375 and A2058 melanoma cells were treated with increasing concentrations of 7-DHC (0, 1, 2.5, 5, 10 and 25 μM) for 48 h. The results revealed that 10 and 25 μM 7-DHC significantly inhibited the proliferation of melanoma cells (Fig. 1A and B), but not that of 293T cells (Fig. S1). Subsequently, Annexin V-FITC and PI staining was used to evaluate the apoptosis rate of A375 and A2058 melanoma cells treated with different concentrations (1, 5 and 10 μM) of 7-DHC. The results of the flow cytometer assay revealed that the proportion of late apoptotic A375 and A2058 cells was markedly increased with the increasing doses of 7-DHC compared with the ethanol control (Fig. 1C and D). In addition, Hoechst/PI double staining assay revealed that 7-DHC induced necrosis in melanoma cells (Fig. S2A). Tumor metastasis is one of the hallmarks of malignant melanoma and is closely associated with a poor prognosis (23). In order to investigate the migration capability of melanoma cells treated with 7-DHC, RTCA assay was used to continuously monitor the cell index value for 36 h, and wound-healing assay was used to detect the cell migration rate. The results of RTCA demonstrated that the cell index of A375 and A2058 cells treated with 25 μM 7-DHC was lower compared with that of cells treated with ethanol or with low concentrations of 7-DHC at 36 h, which demonstrated that only a high concentration (25 μM) of 7-DHC had the ability to inhibit the migration rate of melanoma cells (Fig. 1E and F). Similarly, the wound-healing assay revealed that the migration rate of melanoma cells treated with 7-DHC was lower compared with that of the ethanol control (Fig. S2B), suggesting that the migration of melanoma cells was negatively affected by 7-DHC.

Considering that cell proliferation is regulated by the cell cycle, flow cytometry was used to evaluate any changes in the cell cycle that may lead to apoptosis and low proliferation of melanoma cells. Flow cytometry revealed that the cell cycle of A375 and A2058 melanoma cells treated with 7-DHC was blocked at the S phase in a dose-dependent manner (Fig. S3A-D), which may result in apoptosis of melanoma cells and may limit their proliferation rate.

RNA-seq analysis of melanoma cells treated with 7-DHC. In order to further investigate the mechanism of 7-DHC on inhibiting melanoma, whole transcriptome sequencing of A375 melanoma cells treated with 7-DHC (10 and 25 μM) and ethanol control was performed three times. Significant differential expression of genes in A375 cells treated with 7-DHC versus ethanol control were screened for, revealing an intersection of differentially expressed genes, including 65 downregulated genes and 14 upregulated genes, shown using a Venn diagram and a heatmap in Fig. 2A. Subsequently, RNA-seq of A375 cells treated with 7-DHC was analyzed via GSEA to screen for altered signaling pathways. GSEA results revealed that genes associated with positive regulation of NF-κB import into nucleus and NF-κB signaling were significantly downregulated in A375 cells treated with 7-DHC compared with the ethanol negative control (Fig. 2B). Due to the abnormality of NF-κB signaling, it was postulated that 7-DHC may repress melanoma via NF-κB signaling, and therefore the association between 7-DHC and RELA, an important transcription factor of NF-κB signaling (24), was analyzed. Firstly, combined with the aforementioned RNA-seq results, three RELA-shRNA lentiviruses were infected into A375 cells, revealing that RELA downregulation also decreased the expression levels of target genes (LINC00552, ADAM19 and IGFBP5) of 7-DHC compared with scrambled shRNA (Fig. 2C). Subsequently, ChIP-qPCR of 7-DHC target genes revealed that RELA could bind to the promoters of the aforementioned genes, especially ADAM19 and LINC00522 (Fig. 2D).

7-DHC inhibits melanoma via the Akt1/NF-κB signaling pathway. The abnormal activation of signal transduction caused by somatic mutations is very common in patients with cancer, particularly in those with advanced melanoma (25-28). In order to determine the underlying molecular mechanism of 7-DHC in melanoma, the somatic mutations of kinases, such as Akt1, Akt2 and Akt3, involved in signal transduction were analyzed in 471 patients with melanoma from TCGA database. As shown in Fig. 3A, the mutation rates of Akt1, Akt2 and Akt3, which belong to the PI3K/AKT signaling pathway, and BRAF, upstream of MAPK signaling, were higher compared with kinases from other signaling pathways. The PI3K/AKT and MAPK signaling pathways were chosen to determine the specific effect of 7-DHC via western blotting. Compared with the ethanol negative control, treatment with 7-DHC decreased the protein expression levels of pAkt1-Ser473 rather than those of pAkt-Thr308 or pMEK1 (Figs. 3B and S4A). Furthermore, 7-DHC increased the expression levels of RELA in cytoplasm in melanoma cells, which demonstrated that the inhibition of free RELA translocation into the nucleus (Figs. 3C and S4B) suggested that 7-DHC may promote tumor regression by decreasing NF-κB signaling. To confirm whether 7-DHC also inhibited RELA expression, the luciferase activity in A375 cells treated with various concentrations of 7-DHC was detected, revealing that 7-DHC could inhibit RELA expression in a dose-dependent manner (Fig. 3D). In addition, although the PI3K/AKT signaling pathway is downstream of

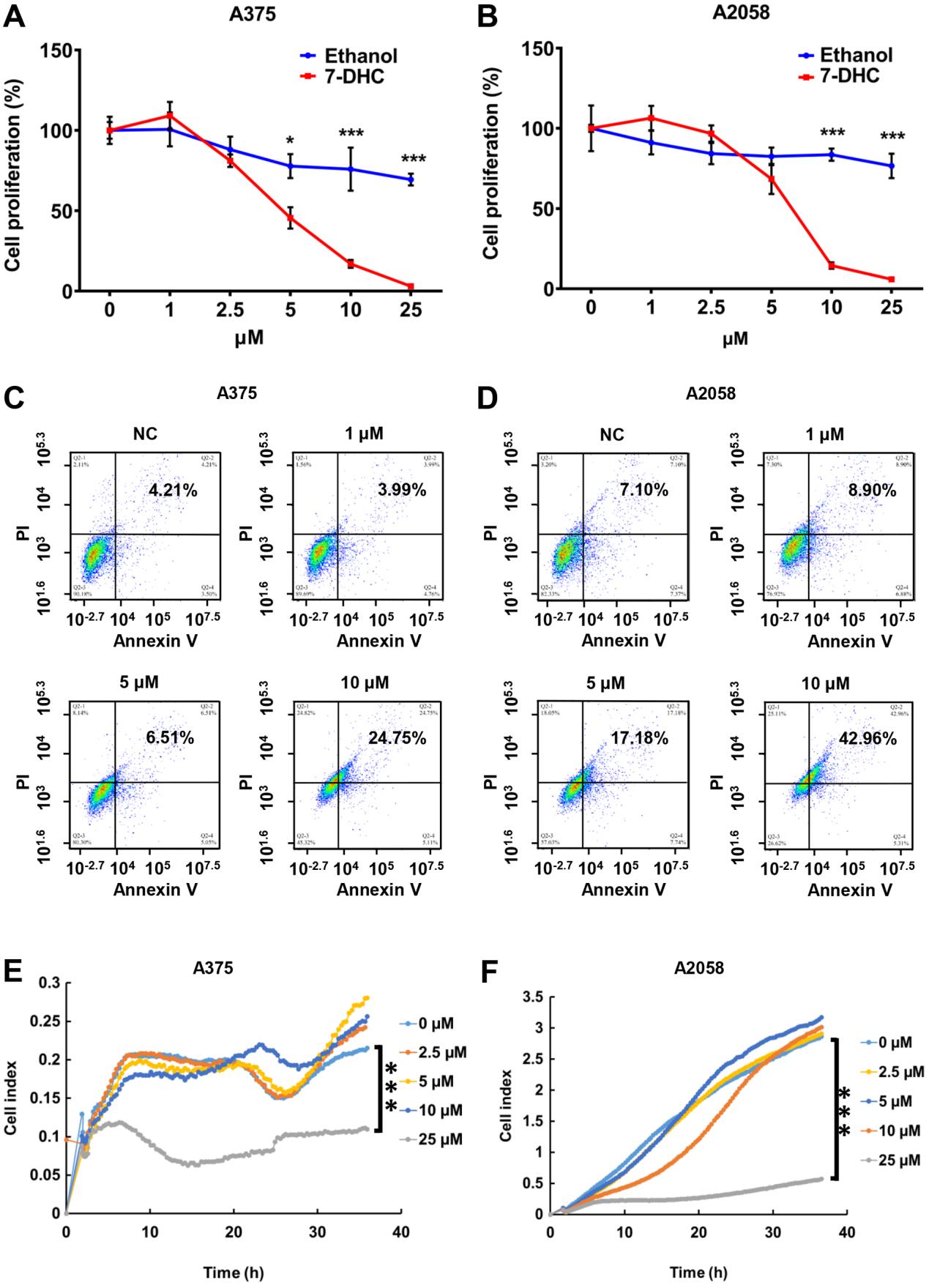

Figure 1. 7-DHC increases apoptosis and inhibits proliferation and migration of melanoma cells. Cell proliferation in (A) A375 and (B) A2058 melanoma cells treated with multiple concentrations (0, 1, 2.5, 5, 10 and 25 μM) of 7-DHC and ethanol as a control for 48 h. Apoptosis of (C) A375 and (D) A2058 melanoma cells treated with 7-DHC (1, 5 and 10 μM) for 48 h was examined using flow cytometry, with ethanol used as a control. Migration of (E) A375 and (F) A2058 melanoma cells treated with 7-DHC (0, 2.5, 5, 10 and 25 μM) was measured via real-time cellular analysis assay. *P<0.05, ***P<0.001. 7-DHC, 7-dehydrocholesterol; NC, negative control.

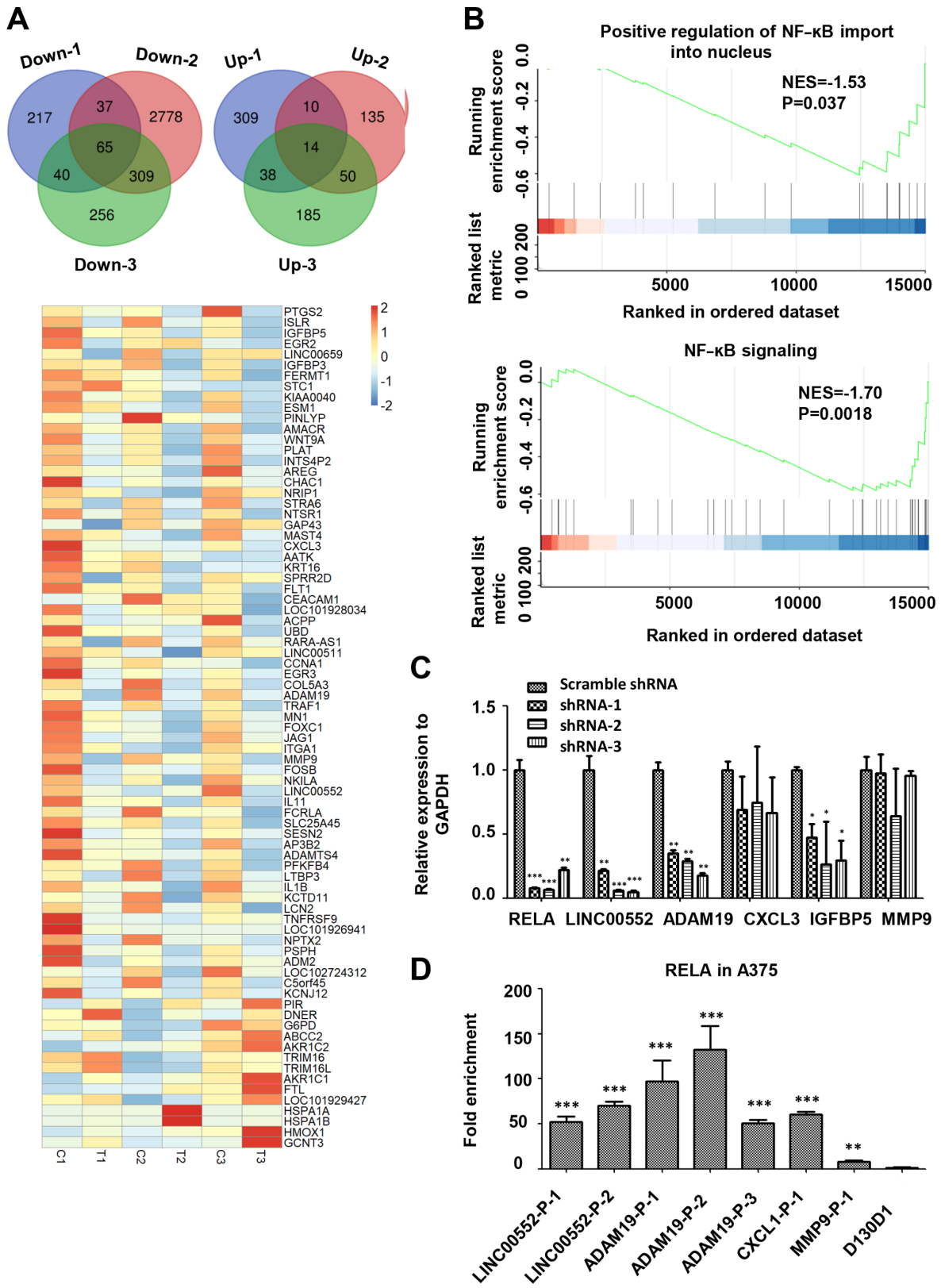

Figure 2. RNA-seq analysis of A375 melanoma cells treated with 7-DHC. (A) Venn diagrams show the intersection of significant differentially expressed genes (upregulated and downregulated) in A375 cells treated with 7-DHC (compared with ethanol) in RNA sequencing performed three times. Heatmap of 79 significant differentially expressed genes in A375 melanoma cells treated with 7-DHC (T1, T2, T3) compared with ethanol control (C1, C2, C3). (B) Gene Set Enrichment Analysis demonstrated the downregulated signaling pathways associated with NF-κB signaling in A375 melanoma cells treated with 7-DHC. (C) Relative expression of 7-DHC target genes (RELA, LINC00552, ADAM19, CXCL3, IGFBP5 and MMP9) in A375 cells infected with RELA-shRNA lentiviruses compared with scrambled shRNA lentiviruses. *P<0.05, **P<0.01, ***P<0.001 vs. scramble shRNA. (D) Chromatin immunoprecipitation-quantitative PCR of RELA bound to different promoter regions of 7-DHC target genes (LINC00552-P-1, LINC00552-P-2, ADAM19-P-1, ADAM19-P-2, ADAM19-P-3, CXCL1-P-1 and MMP9-P-1) and negative control D130D1. D130D1 (negative group) cannot bind to RELA. **P<0.01, ***P<0.001 vs. D130D1. 7-DHC, 7-dehydrocholesterol; shRNA, short hairpin RNA; NES, normalized enrichment score; RELA, RELA proto-oncogene NF-κB subunit; LINC00552, long intergenic non-protein coding RNA 552; ADAM19, ADAM metallopeptidase domain 19; CXCL3, C-X-C motif chemokine ligand 3; IGFBP5, insulin-like growth factor binding protein 5; P-1/2, promoter region 1/2.

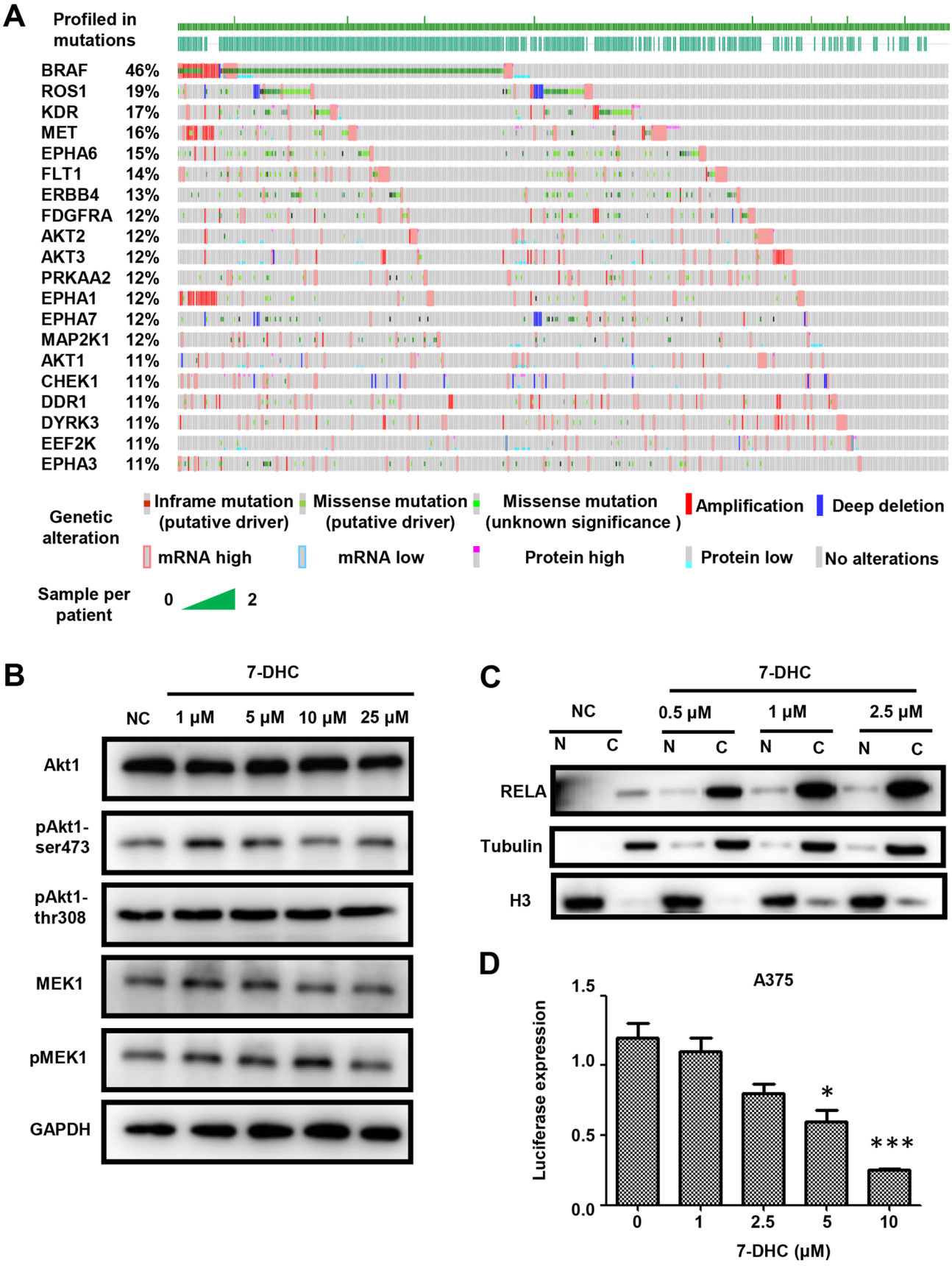

Figure 3. 7-DHC inhibits melanoma via the Akt1/NF-κB signaling pathway. (A) Top 20 somatic mutations of kinases via analyzing The Cancer Genome Atlas-skin cutaneous melanoma dataset. (B) Western blot analysis of A375 cells treated with several concentrations (1, 5, 10 and 25 μM) of 7-DHC were compared with cells treated with ethanol as the NC for the analysis of the levels of pAkt1-Ser473, pAkt1-Thr308/309 and pMEK1 normalized to GAPDH. (C) Western blot analysis of A375 cells treated with several concentrations (0, 0.5, 1 and 2.5 μM) of 7-DHC were compared with cells treated with ethanol as the NC to analyze the entry of RELA into the nucleus. (D) Luciferase expression of A375 cells transfected with 4 repeating motifs of RELA after adding various concentrations (1, 2.5, 5, and 10 μM) of 7-DHC compared with the ethanol negative control (0 μM 7-DHC). *P<0.05, ***P<0.001. 7-DHC, 7-dehydrocholesterol; RELA, RELA proto-oncogene NF-κB subunit; p, phosphorylated; NC, negative control; H3, histone H3; N, nuclear; C, cytoplasmic.

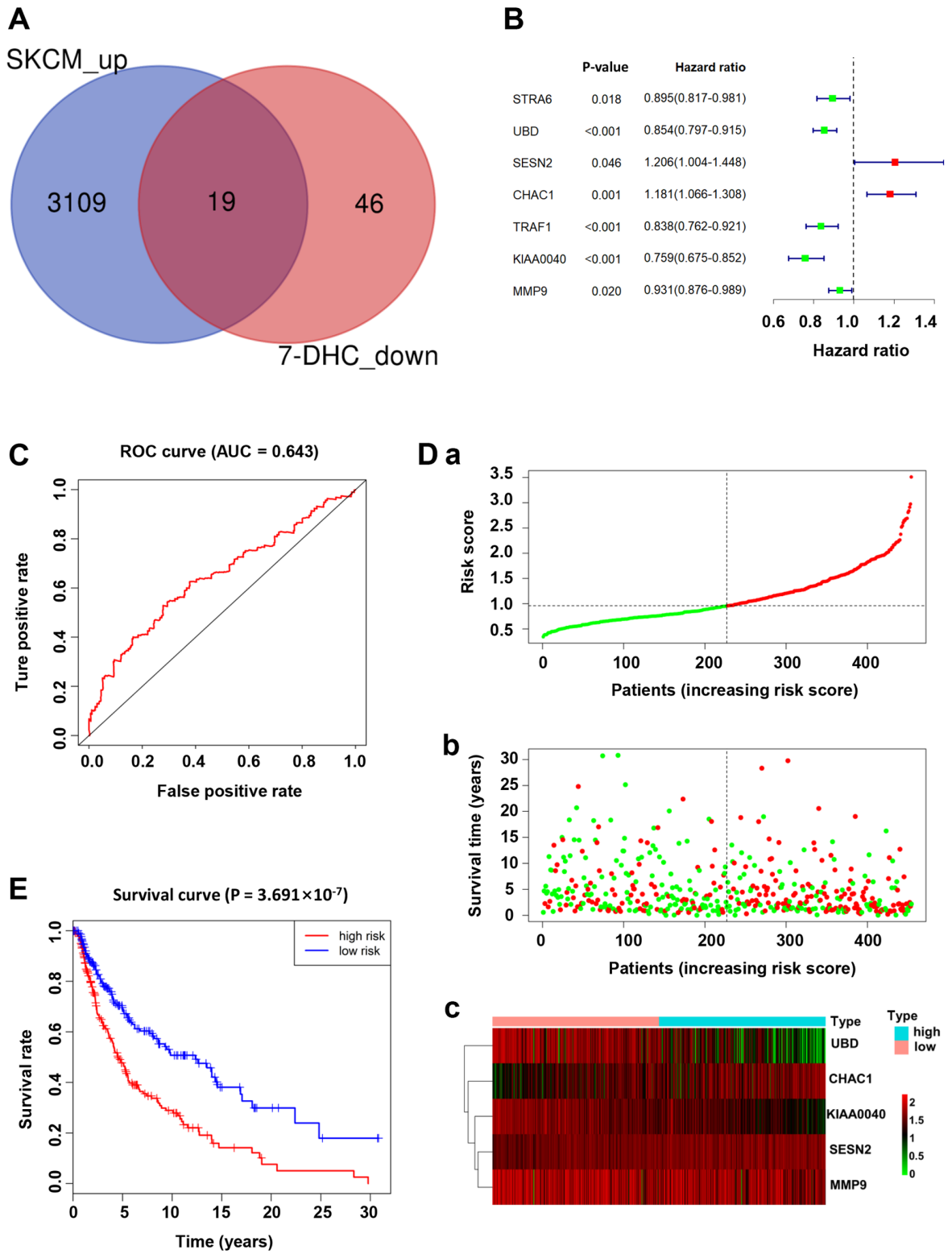

Figure 4. 7-DHC gene signature is associated with a poor prognosis in patients with melanoma. (A) Venn diagram showing the interaction of upregulated genes in The Cancer Genome Atlas-skin cutaneous melanoma dataset and downregulated genes in A375 melanoma cells treated with 7-DHC. (B) Multivariate Cox regression analysis of seven significant genes (STRA6, UBD, SESN2, CHAC1, TRAF1, KIAA0040 and MMP9). (C) ROC curve demonstrating the specificity and selectivity of the gene signature. (D) Distribution of (a) risk scores, (b) survival status and (c) expression levels of five genes of the gene signature with significant upregulated expression. (green and red lines/dots represent low and high risk, respectively). (E) Survival curve of five significant differential genes. 7-DHC, 7-dehydrocholesterol; ROC, receiver operating characteristic; AUC, area under the curve.

the NF-κB signaling pathway, the association between 7-DHC and the two aforementioned signaling pathways was investigated. Therefore, gradient concentrations (0, 1, 5 and 10 μM) of 7-DHC were added to A375 melanoma cells together with 1 μM IGF1, an Akt1 activator, at 37˚C for 48 h, which demonstrated that 7-DHC inhibited the protein expression levels

of pAkt1-Ser473, while addition of IGF1 partially rescued this inhibition (Fig. S4C). Additionally, the Akt1 inhibitors MK-2206 (1 μM at 37˚C for 48 h) and AKT inhibitor III (1 μM at 37˚C for 48 h) were added to A375 and A2058 melanoma cells, and reported RELA target genes were detected via RT-qPCR. The results demonstrated that inhibiting Akt1 could restrain the expression levels of RELA target genes (Fig. S4D and E). In summary, 7-DHC may inhibit melanoma via the Akt1/NF-κB signaling pathway.

7-DHC gene signature is associated with a poor prognosis in patients with melanoma. In order to determine the core target genes of 7-DHC in melanoma combined with prognosis, the clinical data and transcriptome sequencing data of 471 patients with melanoma from TCGA database (TCGA-SKCM) were analyzed. Firstly, 19 genes were obtained by intersecting the downregulated genes in A375 cells treated with 7-DHC and the upregulated genes in patients with melanoma (Fig. 4A). Subsequently, a 7-DHC gene signature associated with prognosis, including STRA6, UBD, SESN2, CHAC1, TRAF1, KIAA0040 and MMP9, was identified based on the prognosis coefficient of the 19 aforementioned genes via univariate Cox proportional hazards regression analysis, which revealed that the 7 genes of the 7-DHC signature may be used as preliminary prognostic factors in patients with melanoma (Fig. 4B). According to the median value of the risk score calculated using the survival R package, patients with melanoma were divided into high- and low-risk groups. The distribution of the risk scores, along with the corresponding OS data and the expression levels of five genes in the 7-DHC gene signature were plotted and shown in Fig. 4D. Patients with higher risk scores tended to experience a shorter OS time and a higher death rate compared with those with lower risk scores. The 5-gene signature, including UBD, CHAC1, KIAA0040, SESN2 and MMP9, was constructed to provide the guideline for prognosis, which demonstrated that the higher the expression levels of CHAC1, KIAA0040, SESN2 and MMP9, the higher the risk score, while the lower the expression levels of UBD, the lower the risk score in patients with melanoma (Fig. 4D). In addition, ROC analysis was used to estimate the significance of the five genes in the gene signature, and the area under the curve value of the ROC analysis for the prognostic signature was 0.643 (Fig. 4C). To assess the overall prognosis of the five genes in the prognosis model, Kaplan-Meier analysis revealed that a higher risk score was associated with a higher mortality risk (Fig. 4E).

Discussion

Mammalian cholesterol synthesis is one of the most complicated biological processes that includes 21 enzymatic steps that generate numerous cholesterol metabolites (29). The dysregulation of cholesterol synthesis is implicated in the progression of hypocholesterolemia, hypercholesteremia and diabetes (30-32). Furthermore, metabolites in cholesterol metabolism, both in synthesis and in metabolism and transport, have been demonstrated to promote or delay tumorigenesis and metastasis (33,34). For example, it has been demonstrated that glucocorticoids and Dendrogenin A function as tumor suppressors to slow tumor growth and increase cell apoptosis in breast cancer (33). Additionally, a previous study revealed that 7-DHC had a cytotoxic effect on melanoma cell lines (20), but the mechanism of 7-DHC in melanoma cells is poorly understood.

The present data confirmed the antitumor property of 7-DHC in inducing apoptosis and inhibiting proliferation and metastasis in A375 and A2058 melanoma cells. To uncover the molecular mechanism underlying the anticancer property of 7-DHC, according to RNA-seq data, GSEA demonstrated that the downregulated genes were associated with the PI3K-AKT and NF-κB signaling pathways. Consistently, the top 20 most frequent somatic mutations of kinase-coding genes were analyzed, revealing that AKT1, AKT2 and AKT3 in the PI3K/AKT signaling pathway, and BRAF in the MAPK signaling pathway were the most frequent hotspots of mutations in patients with melanoma. Subsequent validation demonstrated that 7-DHC restrained melanoma via decreasing the phosphorylation levels of Akt1-Ser473 and further blocked the translocation into the nucleus of free RELA. Furthermore, 7-DHC decreased the expression levels of RELA as assessed via the luciferase assay. Therefore, it can be concluded that 7-DHC may repress melanoma via the Akt1/NF-κB signaling pathway. Subsequently, a 7-DHC gene signature was established via univariate and multivariate Cox proportional hazards regression analysis, including five prognosis-dependent genes identified by combining RNA-seq data from melanoma cell lines with expression data from patients in the TCGA-SKCM dataset.

In conclusion, compared with a previous study demonstrating the inhibitory effect of 7-DHC in melanoma cells (20), the molecular mechanism of the antitumor effect of 7-DHC was further investigated in the present study. The present findings provide a molecular basis for 7-DHC as a potential novel anti-neoplastic drug. The anticancer properties of 7-DHC were analyzed in A375 and A2058 melanoma cells, demonstrating that 7-DHC promoted the regression of melanoma by decreasing the phosphorylation levels of Akt1 rather than those of MEK1, and by inhibiting the nuclear translocation of RELA. Furthermore, the 7-DHC gene signature of genes that were downstream of 7-DHC was identified, which was negatively associated with the survival of patients with melanoma. The present findings shed light on the molecular mechanism of 7-DHC in melanoma and provide a theoretical basis for its clinical application. Although the mechanism of 7-DHC inhibiting melanoma was elucidated in the present study, future studies should perform further *in vivo* and clinical experiments of the effect of 7-DHC in treating melanoma.

Acknowledgements

Not applicable.

Funding

The present study was supported by the Natural Science Foundation of Tianjin City (grant no. 18JCQNJC13300) and the National Natural Science Foundation of China (grant no. 81700153).

Availability of data and materials

The datasets used and/or analyzed during the current study are available from the corresponding author on reasonable request.

Authors' contributions

BL, CL and YY conceived and supervised the study. BL and JL designed the experiments. JL, FZ, RZ, LC and JQ performed the experiments. JL, LY, TC, YH, YW, MY and WX analyzed the data. BL, CL and YY wrote the manuscript. All authors read and approved the final version of manuscript.

Ethics approval and consent to participate

Not applicable.

Patient consent for publication

Not applicable.

Competing interests

The authors declare that they have no competing interests.

References

1. Schadendorf D, van Akkooi ACJ, Berking C, Griewank KG, Gutzmer R, Hauschild A, Stang A, Roesch A and Ugurel S: Melanoma. Lancet 392: 971-984, 2018.
2. Ferlay J, Soerjomataram I, Dikshit R, Eser S, Mathers C, Rebelo M, Parkin DM, Forman D and Bray F: Cancer incidence and mortality worldwide: Sources, methods and major patterns in GLOBOCAN 2012. Int J Cancer 136: E359-E386, 2015.
3. Leong SP, Mihm MC Jr, Murphy GF, Hoon DS, Kashani-Sabet M, Agarwala SS, Zager JS, Hauschild A, Sondak VK, Guild V and Kirkwood JM: Progression of cutaneous melanoma: Implications for treatment. Clin Exp Metastas 29: 775-796, 2012.
4. Crocetti E, Mallone S, Robsahm TE, Gavin A, Agius D, Ardanaz E, Lopez MC, Innos K, Minicozzi P, Borgognoni L, *et al*: Survival of patients with skin melanoma in Europe increases further: Results of the EUROCARE-5 study. Eur J Cancer 51: 2179-2190, 2015.
5. Whiteman DC, Pavan WJ and Bastian BC: The melanomas: A synthesis of epidemiological, clinical, histopathological, genetic, and biological aspects, supporting distinct subtypes, causal pathways, and cells of origin. Pigment Cell Melanoma Res 24: 879-897, 2011.
6. Pennello G, Devesa S and Gail M: Association of surface ultraviolet B radiation levels with melanoma and nonmelanoma skin cancer in United States blacks. Cancer Epidemiol Biomarkers Prev 9: 291-297, 2000.
7. Rodriguez-Cerdeira C, Gregorio MC, López-Barcenas A, Sánchez-Blanco E, Sánchez-Blanco B, Fabbrocini G, Bardhi B, Sinani A and Guzman RA: Advances in immunotherapy for melanoma: A comprehensive review. Mediators Inflamm 2017: 3264217, 2017.
8. Shain AH, Yeh I, Kovalyshyn I, Sriharan A, Talevich E, Gagnon A, Dummer R, North J, Pincus L, Ruben B, *et al*: The genetic evolution of melanoma from precursor lesions. N Engl J Med 373: 1926-1936, 2015.
9. Guo D, Lui GYL, Lai SL, Wilmott JS, Tikoo S, Jackett LA, Quek C, Brown DL, Sharp DM, Kwan RYQ, *et al*: RAB27A promotes melanoma cell invasion and metastasis via regulation of pro-invasive exosomes. Int J Cancer 144: 3070-3085, 2019.
10. Michielin O, van Akkooi ACJ, Ascierto PA, Dummer R and Keilholz U; ESMO Guidelines Committee. Electronic address: clinicalguidelines@esmo.org: Cutaneous melanoma: ESMO clinical practice guidelines for diagnosis, treatment and follow-up†. Ann Oncol 30: 1884-1901, 2019.
11. Duggan MA, Anderson WF, Altekruse S, Penberthy L and Sherman ME: The surveillance, epidemiology, and end results (SEER) program and pathology: Toward strengthening the critical relationship. Am J Surg Pathol 40: e94-e102, 2016.
12. Flaherty KT: Narrative review: BRAF opens the door for therapeutic advances in melanoma. Ann Intern Med 153: 587-591, 2010.
13. Menzies AM and Long GV: Systemic treatment for BRAF-mutant melanoma: Where do we go next? Lancet Oncol 15: E371-E381, 2014.
14. Korman JB and Fisher DE: Developing melanoma therapeutics: Overview and update. Wiley Interdiscip Rev Syst Biol Med 5: 257-271, 2013.
15. Prabhu AV, Luu W, Sharpe LJ and Brown AJ: Cholesterol-mediated degradation of 7-dehydrocholesterol reductase switches the balance from cholesterol to vitamin D synthesis. J Biol Chem 291: 8363-8373, 2016.
16. Piotrowska A, Wierzbicka J and Żmijewski MA: Vitamin D in the skin physiology and pathology. Acta Biochim Pol 63: 17-29, 2016.
17. Xiao J, Li W, Zheng X, Qi L, Wang H, Zhang C, Wan X, Zheng Y, Zhong R, Zhou X, *et al*: Targeting 7-dehydrocholesterol reductase integrates cholesterol metabolism and IRF3 activation to eliminate infection. Immunity 52: 109-122.e6, 2020.
18. Wang Y, Tian N, Li C, Hou Y, Wang X and Zhou Q: Incorporation of 7-dehydrocholesterol into liposomes as a simple, universal and efficient way to enhance anticancer activity by combining PDT and photoactivated chemotherapy. Chem Commun (Camb) 55: 14081-14084, 2019.
19. Tian NN, Li C, Tian N, Zhou QX, Hou YJ, Zhang BW and Wang XS: Syntheses of 7-dehydrocholesterol peroxides and their improved anticancer activity and selectivity over ergosterol peroxide†. New J Chem 41: 14843-14846, 2017.
20. Gelzo M, Granato G, Albano F, Arcucci A, Dello Russo A, De Vendittis E, Ruocco MR and Corso G: Evaluation of cytotoxic effects of 7-dehydrocholesterol on melanoma cells. Free Radical Bio Med 70: 129-140, 2014.
21. Livak KJ and Schmittgen TD: Analysis of relative gene expression data using real-time quantitative PCR and the 2(-Delta Delta C(T)) method. Methods 25: 402-408, 2001.
22. Yu G, Wang LG, Han Y and He QY: clusterProfiler: An R package for comparing biological themes among gene clusters. OMICS 16: 284-287, 2012.
23. Chistiakov DA and Chekhonin VP: Circulating tumor cells and their advances to promote cancer metastasis and relapse, with focus on glioblastoma multiforme. Exp Mol Pathol 105: 166-174, 2018.
24. Kaltschmidt B, Greiner JFW, Kadhim HM and Kaltschmidt C: Subunit-specific role of NF-κB in cancer. Biomedicines 6: 44, 2018.
25. Hinz N and Jücker M: Distinct functions of AKT isoforms in breast cancer: A comprehensive review. Cell Commun Signal 17: 154, 2019.
26. Wise HM, Hermida MA and Leslie NR: Prostate cancer, PI3K, PTEN and prognosis. Clin Sci (Lond) 131: 197-210, 2017.
27. Tilborghs S, Corthouts J, Verhoeven Y, Arias D, Rolfo C, Trinh XB and van Dam PA: The role of nuclear factor-kappa B signaling in human cervical cancer. Crit Rev Oncol Hematol 120: 141-150, 2017.
28. Atefi M, Avramis E, Lassen A, Wong DJ, Robert L, Foulad D, Cerniglia M, Titz B, Chodon T, Graeber TG, *et al*: Effects of MAPK and PI3K pathways on PD-L1 expression in melanoma. Clin Cancer Res 20: 3446-3457, 2014.
29. Silvente-Poirot S and Poirot M: Cancer. Cholesterol and cancer, in the balance. Science 343: 1445-1446, 2014.
30. Moutzouri E, Elisaf M and Liberopoulos EN: Hypocholesterolemia. Curr Vasc Pharmacol 9: 200-212, 2011.
31. Bentz MH and Magnette J: Hypocholesterolemia in the acute phase of inflammation during sepsis. Rev Med Int 19: 168-172, 1998.
32. Mokdad AH, Bowman BA, Ford ES, Vinicor F, Marks JS and Koplan JP: The continuing epidemics of obesity and diabetes in the United States. JAMA 286: 1195-1200, 2001.
33. de Medina P, Paillasse MR, Segala G, Voisin M, Mhamdi L, Dalenc F, Lacroix-Triki M, Filleron T, Pont F, Saati TA, *et al*: Dendrogenin A arises from cholesterol and histamine metabolism and shows cell differentiation and anti-tumour properties. Nat Commun 4: 1840, 2013.
34. Wu Q, Ishikawa T, Sirianni R, Tang H, McDonald JG, Yuhanna IS, Thompson B, Girard L, Mineo C, Brekken RA, *et al*: 27-Hydroxycholesterol promotes cell-autonomous, ER-positive breast cancer growth. Cell Rep 5: 637-645, 2013.